

# MEMS Gyroscope with Interchangeable Modalities of Operation

Alexander A. Trusov, Igor P. Prikhodko, Sergei A. Zotov, and Andrei M. Shkel  
MicroSystems Laboratory, University of California, Irvine, CA, USA

**Abstract**—We present a silicon MEMS Coriolis vibratory gyroscope capable to measure the angular rate and angle of rotation, both in amplitude modulation (AM) and frequency modulation (FM) arrangement. The approach takes advantage of the symmetric quadruple mass gyroscope (QMG) architecture with maximized quality (Q) factors and isotropy of both the resonant frequency and damping, with measured 1.2 million Q-factor (1% split) and 2 kHz frequency (0.1% split). The vacuum sealed SOI gyroscope experimentally demonstrated a 0.8 °/hr bias instability in rate measuring mode, a 18,000 °/s linear input range, and a 100 Hz measurement bandwidth (limited by the setup) in both whole-angle mode and FM arrangement. Temperature characterization of the transducer also revealed less than 0.2% variation of the angular rate response between 25 °C and 70 °C environments, enabled by the self-calibrating differential frequency detection. Interchangeable operation of the QMG transducer provides a measured 157 dB dynamic range with a 210 dB fundamental limit for a 2 kHz transducer, making one high-Q mechanical structure suitable for demanding high precision and wide input range applications.

## I. INTRODUCTION

Majority of commercial MEMS vibratory gyroscopes are angular rate measuring sensors, which employ energy transfer between the two modes of vibration in response to the inertial rotation [1], [2]. While the angular rate information with moderate accuracy is sufficient for the motion detection and stabilization in consumer electronics and automotive safety devices, the precision angular position and continuous orientation tracking is required for inertial navigation, North tracking, dead-reckoning, and targeting systems [3]. Moreover, the wide input range and high measurement bandwidth are also critical for pointing and missile guidance systems, especially in harsh and GPS-denied environments. Although conventional fiber optic, ring laser, and hemispherical resonator gyroscopes can in principle satisfy some of the requirements, their further miniaturization is challenging. The emergence of silicon microelectromechanical (MEMS) gyroscopes capable of precision and wide dynamic range measurements of both angular velocity and position (angle) is highly desirable. Although few authors report feasibility of precision rate gyroscopes with a sub-degree per hour bias instability [4]–[7], inertial MEMS are yet to break into a high-precision market [8].

The challenge for implementation is the requirement for high quality (Q) factors, as well as structural isotropy of stiffness and damping. Recently, we proposed the interchangeable rate and rate integrating (whole-angle) operation [9], making one high-Q transducer suitable for high precision and wide range measurements. Using the same transducer we also

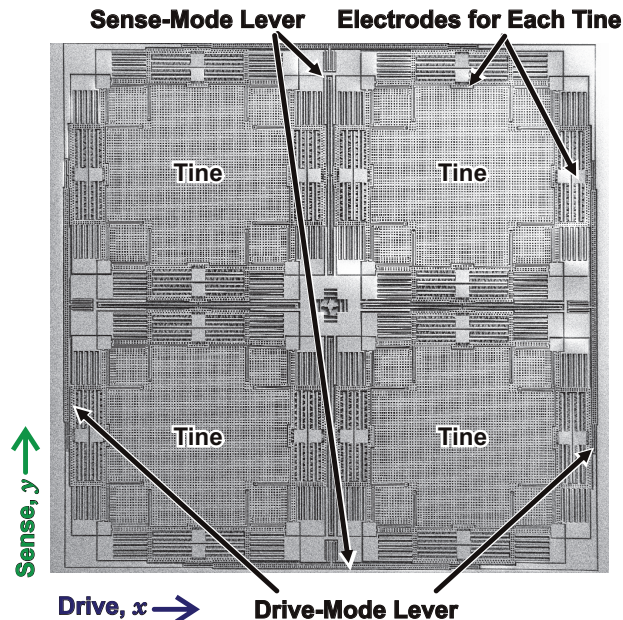


Fig. 1. SEM image of a fabricated 100  $\mu\text{m}$  SOI quadruple mass gyroscope (QMG). Die size is 8.6  $\times$  8.6 mm.

demonstrated a sub-degree per hour rate resolution [7], high input range and measurement bandwidth [10], [11], as well as a differential frequency detection robust to the temperature variations [12]. In this paper we review each of the operation mode and propose an interchangeable operation for the realization of a precision and high dynamic range silicon MEMS sensor with digital output for demanding inertial navigation and guidance applications.

In the following sections we describe the gyroscope dynamics, design requirements, and experimental characterization for the each mode of operation, i) conventional amplitude modulation (AM), ii) whole-angle (WA), and iii) frequency modulation (FM). Using the same high-Q transducer structure, Fig. 1, for all experiments we demonstrated operation of each mode by switching the signal conditioning and control electronics.

## II. TRANSDUCER DESIGN AND FABRICATION

In this section we report the transducer design, fabrication, and structural characterization.

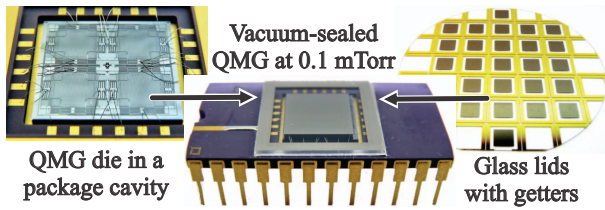


Fig. 2. Photograph of a vacuum packaged QMG used in the experiments. Insets: die before sealing; glass lid wafer.

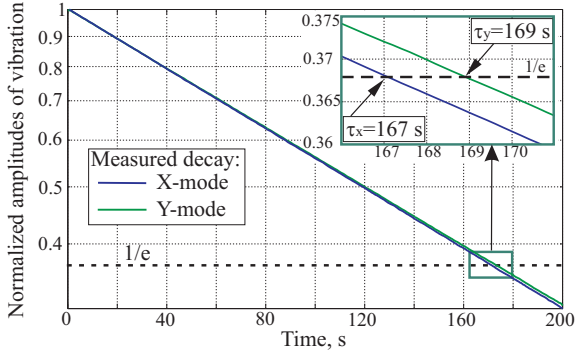


Fig. 3. Experimental characterization of the vacuum packaged QMG using ring-down tests, revealing closely matched drive- and sense-mode  $Q$ -factors of 1.16 million (with  $\Delta Q/Q$  of 1 %).

#### A. Design Criteria

Several design criteria must be met by the mechanical sensor element to fully realize the proposed methods of operation. A geometrically symmetric and mode-matched structure is needed to optimize the minimal detectable angular rate signal and increase the temperature stability of the sensor. High  $Q$ -factors allow achieving high rate resolution and frequency stability. Identical high  $Q$  is needed in both modes of mechanical vibration to maximize the rate resolution and enable low angle drift. These requirements are satisfied by an X-Y symmetric, dynamically balanced, anti-phase operated gyroscope, such as the recently introduced quadruple mass gyroscope (QMG) architecture [13].

#### B. Quadruple Mass Gyroscope Architecture

The mechanical structure of the QMG mechanical sensor element comprises four identical, symmetrically decoupled tines with linear coupling flexures as well as a pair of anti-phase synchronization lever mechanisms for both the X- and the Y-mode, Fig. 1. This X-Y symmetric system of four anti-phase tines provides the structure with two anti-phase, dynamically balanced modes of mechanical vibration at a single operational frequency. The complete X-Y structural symmetry of the device improves robustness against the fabrication imperfections and temperature induced frequency drifts. An additional advantage of the QMG anti-phase levered architecture is the mechanical suppression of the parasitic common mode in-phase displacement in the coupled tines. The same QMG architecture will be used for all three modes of operation reported in this paper.

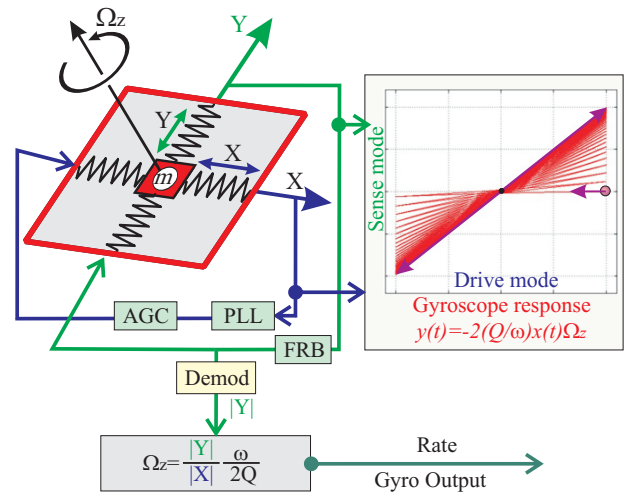


Fig. 4. Schematic and operating principle of a gyroscope for angular rate measurements (conventional amplitude modulation mode of operation). The axis of vibration is locked to the intended drive direction. The inertial rotation induces the motion in the sense direction, with the amplitude proportional to an input angular rate.

#### C. Fabrication and Packaging

The QMG prototypes, Fig. 2, were fabricated using an in-house, wafer-level, single-mask process based on silicon-on-insulator (SOI) substrates with 100  $\mu\text{m}$  thick device layer and a 5  $\mu\text{m}$  buried oxide layer. Sensors were defined in a highly doped (boron concentrations of  $10^{20} \text{ cm}^{-3}$ ) device layer by DRIE. Stand-alone ultra-high  $Q$  sensors were obtained by using a package-level technology for robust vacuum sealing [14]. First, the gyroscope die was attached to ceramic package using eutectic solder, and then wire bonded. The device was sealed at sub-mTorr vacuum, preceded by a getter activation on a glass lid.

#### D. Structural characterization

The dynamically balanced, geometrically symmetric design of the QMG is expected to provide closely matched  $Q$ -factors. The damping symmetry of a stand-alone QMG prototype was investigated using ring-down tests. The time-domain amplitude decays of X- and Y-modes were fitted with exponential decays to extract time constants  $\tau$  of 167 s and 169 s, respectively, Fig. 3. The  $Q$ -factors were calculated according to  $Q = \pi f_n \tau$ , with natural frequencies  $f_n$  of approximately 2.2 kHz, Fig. 3. Experimentally measured X-mode  $Q$  of 1.155 and Y-mode  $Q$  of 1.17 million approach the fundamental thermoelastic limit of 1.3 million. The data confirms the design hypothesis of the inherent  $Q$ -factor symmetry in QMG structures.

### III. CONVENTIONAL ANGULAR RATE MODE

This section describes dynamics and experimental characterization of the QMG sensor operated in conventional rate measuring mode [7]. The operating principle is based on amplitude modulation of an input rate employed in most commercially available MEMS rate sensors. The dynamic analysis below assumes that gyroscopes are 2-D isotropic

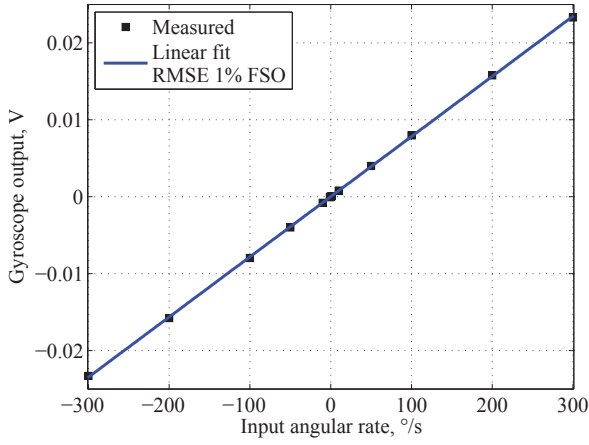


Fig. 5. Measured response of the QMG sensor in rate measuring mode, revealing a  $\pm 300$   $^{\circ}/s$  input range with 1% RMS nonlinearity of FSO.

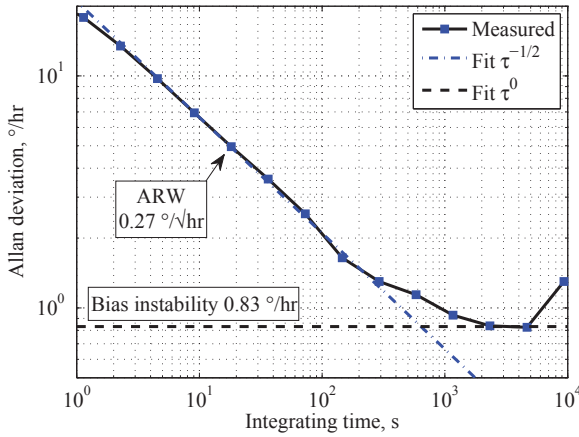


Fig. 6. Allan deviation of the QMG sensor in rate measuring mode, revealing a  $0.27$   $^{\circ}/\sqrt{\text{hr}}$  ARW, and a  $0.8$   $^{\circ}/\text{hr}$  bias instability.

mass-spring-damper systems with the natural frequency  $\omega$  and the quality factor  $Q$ .

### A. Principle of Operation

In the conventional angular rate mode of operation, the  $z$ -axis gyroscope is continuously driven by a force  $f_x \sin(\omega t)$  into a steady-state resonant motion in the drive direction ( $x$ -axis), Fig. 4. The driving voltages are imposed across the differential lateral comb electrodes of the drive-mode shuttles, Fig. 1. The rotation around the  $z$ -axis induces the motion in the sense direction ( $y$ -axis), with the amplitude proportional to an input angular rate  $\Omega_z$ . Sense-mode vibrations are detected using differential parallel plate electrodes of the sense-mode shuttles. For the open-loop operation (at slow angular rates), the amplitude of  $y$  motion is small compared to  $x$  amplitude, and the equations of motion are:

$$\begin{aligned} \ddot{x} + \frac{\omega}{Q}\dot{x} + \omega^2 x &= f_x \sin(\omega t), \\ \ddot{y} + \frac{\omega}{Q}\dot{y} + \omega^2 y &= -2\dot{x}\Omega_z. \end{aligned} \quad (1)$$

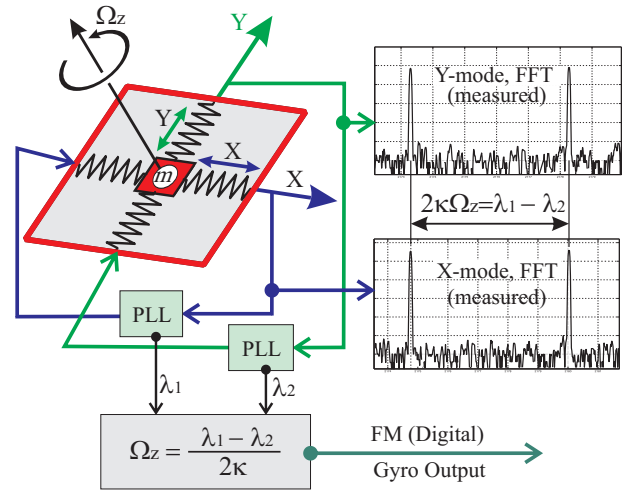


Fig. 7. Schematic and operating principle of a gyroscope for wide range angular rate measurements (frequency modulation mode of operation). The operation is based on the mechanical frequency modulation of the inertial input. The input rotation causes a frequency split between the gyroscope's X-mode and Y-mode, producing a FM measure of the input rate.

The drive-mode can be thought of a simple resonator continuously operated at resonance with a constant amplitude of motion, while the sense-mode is kept unconstrained. The estimate of an inertial stimulus is obtained by demodulating the sense-mode output ( $y$  motion):

$$\Omega_z = \frac{|y|}{|x|} \frac{\omega}{2Q}, \quad (2)$$

and the gyroscope sensitivity to an input rotation can be enhanced by maximizing the  $Q$ -factor or reducing the natural frequency  $\omega$ . This mode of operation tend to provide excellent noise characteristics and a high resolution of angular rate since the axis of vibration is effectively locked to the intended drive direction, as well as controlled by phase locked loop (PLL), automatic gain control (AGC), or alternative controls [15]. On the other hand, the constrained motion along the drive direction often imposes limitations on a rate range and a response time (rate measurement bandwidth). While bandwidth constraints can be eliminated by operating sense-mode in closed-loop force-to-rebalance (FRB) regime, the range limitations can be resolved by switching to FM or WA operating modes. The switching logic implementation for MEMS gyroscopes can be found in [16].

### B. Experimental Characterization of Rate Measuring Mode

The low dissipation QMG sensor operated in rate measuring mode is expected to provide a low noise performance. The packaged QMG sensor with a 2 kHz resonant frequency and a  $0.5$   $\mu\text{m}$  amplitude of motion in the drive mode performed under a 3.6 Hz frequency mismatch between the sense- and drive-modes. The input-output relationship demonstrates a linear rate response in  $\pm 300$   $^{\circ}/s$  input range with 1% RMSE of a full scale output (FSO), Fig. 5.

The QMG noise performance was evaluated using the Allan deviation analysis. The zero rate output of the QMG sense-mode was recorded for 12 hours at a sampling rate of 28 Hz, Fig. 6. Fit to the  $\tau^{-1/2}$  slope (white noise) at the short integration time revealed a  $16.2^\circ/\text{hr}/\sqrt{\text{Hz}} = 0.27^\circ/\sqrt{\text{hr}}$  Angle Random Walk (ARW). The flicker noise reached for integration times between 2500 and 5000 s indicated a  $0.83^\circ/\text{hr}$  bias instability. For times longer than 5000 s the output was dominated by the  $1/f^2$  random walk.

The measured  $0.8^\circ/\text{hr}$  minimal resolution and the 300 % maximum input of the QMG sensor partially satisfy the requirements for tactical-grade gyroscopes, providing a dynamic range of 123 dB. Further performance enhancement is possible by matching the natural frequencies of the drive- and sense-modes [4], [17]. Next, we demonstrate that using physically the same mechanical element, the significantly wider range can be obtained by operating in frequency modulated detection mode with inherent resistance to temperature variations and external shocks.

#### IV. FREQUENCY MODULATED MODE

This section describes dynamics and experimental characterization of the QMG sensor operated in wide range angular rate measuring mode. The operating principle is based on mechanical frequency modulation of an input rate previously introduced in [12].

##### A. Frequency Based Detection of Input Rate

The QMG rate sensor in frequency modulation operation could eliminate the gain-bandwidth and dynamic range trade-off of conventional AM gyroscopes and enable signal-to-noise ratio improvements by taking advantage of high-Q mechanical element without limiting the measurement bandwidth. In contrast to conventional rate measuring mode, the dynamics of FM-operated gyroscope is based on free vibrations of the inertial mass, when both X- and Y-modes are unconstrained and allowed to move freely in response to the inertial stimulus. The free vibrations dynamic of a 2-D isotropic mass-spring-damper system with the natural frequency  $\omega$  and the quality factor  $Q$  in the non-inertial coordinate frame (device frame)  $Oxy$  is (Fig. 7):

$$\begin{aligned} \ddot{x} + \frac{\omega}{Q}\dot{x} + (\omega^2 - \Omega_z^2)x - \dot{\Omega}_z y &= 2\dot{y}\Omega_z, \\ \ddot{y} + \frac{\omega}{Q}\dot{y} + (\omega^2 - \Omega_z^2)y + \dot{\Omega}_z x &= -2\dot{x}\Omega_z. \end{aligned} \quad (3)$$

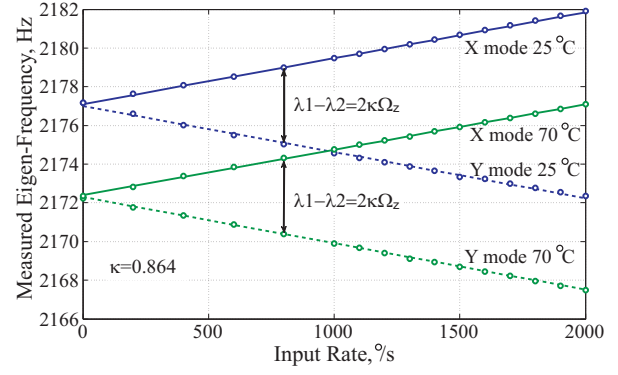
The centrifugal and angular acceleration terms are included to accommodate for fast and wide range input rotations. Assuming negligible damping ( $Q > 10^6$ ), the closed-form solution is:

$$\begin{aligned} x &= A \cos \lambda_1 t + B \cos \lambda_2 t, \\ y &= -A \sin \lambda_1 t + B \sin \lambda_2 t, \end{aligned} \quad (4)$$

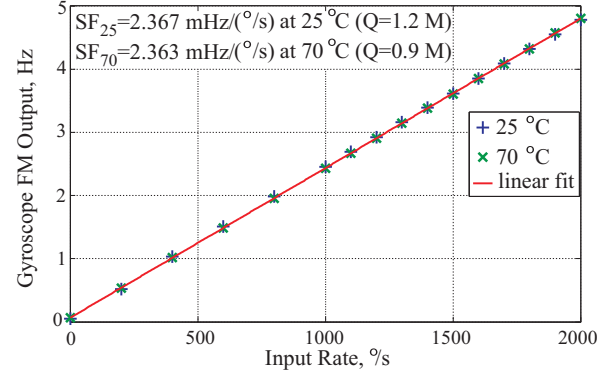
where

$$\lambda_1 = \omega + \Omega_z, \quad \lambda_2 = \omega - \Omega_z \quad (5)$$

are the effective modal frequencies with respect to the rotating reference frame  $Oxy$  in presence of inertial rotation. In the



(a) Differential FM detection of the input rate from the modal frequency split ( $\lambda_1 - \lambda_2$ ) is invariant to temperature.



(b) Measured FM rate responses for 25 °C and 70 °C using differential detection of the modal frequency split with inherent self-calibration.

Fig. 8. Rate characterization of the FM-based sensor shows no drift in the response for 25 °C and 70 °C despite a 30 % reduction in Q-factor and a 5 Hz drop of nominal frequency (without any temperature compensation).

inertial frame of reference, the gyroscope's vibrations contain only one frequency  $\omega$ ; while in the device moving frame  $Oxy$  there are two splitting frequencies  $\lambda_{1,2}$  (4), Fig. 7. The frequency modulation effect (5) is inherent to the moving reference frame and enables angular rate measurements by observing frequency spectrum  $\lambda_{1,2}$  of a sensor according to

$$\Omega_z = (\lambda_1 - \lambda_2)/2. \quad (6)$$

Analysis of Eq. (4) also shows that a vibration pattern in  $x, y$  plane remains stationary in the inertial frame, thereby providing a reference for direct angle measurements [11] (see Section V). The frequency output (6) of a FM sensor can be also easily digitized without consuming A/D conversion resources. At the same time, FM sensor architecture is known to provide inherent robustness against mechanical and electromagnetic interferences (EMI) [18], [19].

##### B. Experimental Characterization of FM Operation

In conventional AM mode, drift of resonant frequency and Q-factors are major sources of scale factor variations and bias drifts over temperature. Theoretical analysis of the proposed FM rate sensor suggest immunity against these drift mechanisms by virtue of the differential frequency detection, i.e.

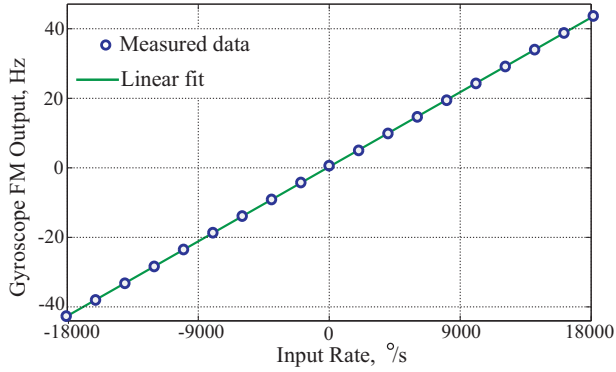


Fig. 9. Characterization of the FM-based rate sensor reveals less than 0.2 % of nonlinearity in wide input range of 18,000 %/s.

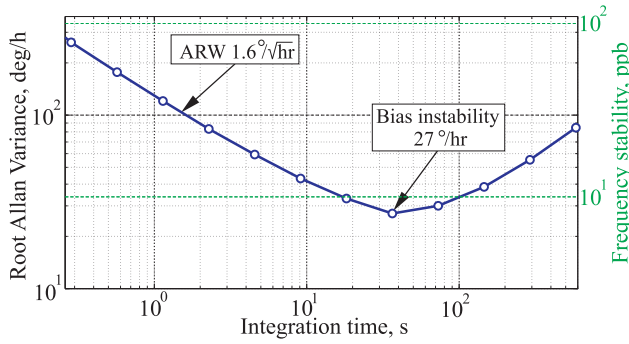


Fig. 10. Measured Allan variance of the FM sensor showing 1.6 %/hr ARW and 27 %/hr bias instability. For the measured 27 %/hr minimal resolution and the 18,000 %/s maximal input, the dynamic range is  $\sim 130$  dB.

by measuring the frequency (6). To experimentally investigate this hypothesis, a vacuum packaged QMG sensor operated in FM mode was characterized on a temperature controlled Ideal Aeromsmith 1291BR rate table at 25 °C and at 70 °C. For these experiments, the X- and Y- modes of the QMG device were electrostatically excited into resonances using a combination of 0.1 Vdc bias and 0.1 Vac driving signals produced by digital PLLs. The motional signals for both modes of vibration were detected using capacitive detection with electromechanical amplitude modulation (EAM). The two modal frequencies of the gyroscope mechanical structure were continuously monitored by the two PLLs, Fig. 7.

As it is theoretically expected for a mode-matched gyroscope, the measured split between the nominally equal modal frequencies was directly proportional to the input rate, Fig. 8(a). Unlike the conventional AM approach, the FM detection of the input rate from the modal frequency split demonstrated invariance to changes in temperature and Q-factors, Fig. 8(b). Without any active temperature compensation, experimental characterization of the FM angular rate sensor at 25 °C and 70 °C revealed less than 0.2% response fluctuation despite a 30 % reduction of the Q-factor and a 5 Hz drop of the nominal frequency (caused by temperature dependency of Young’s modulus).

The proposed FM gyroscope operation also suggests a

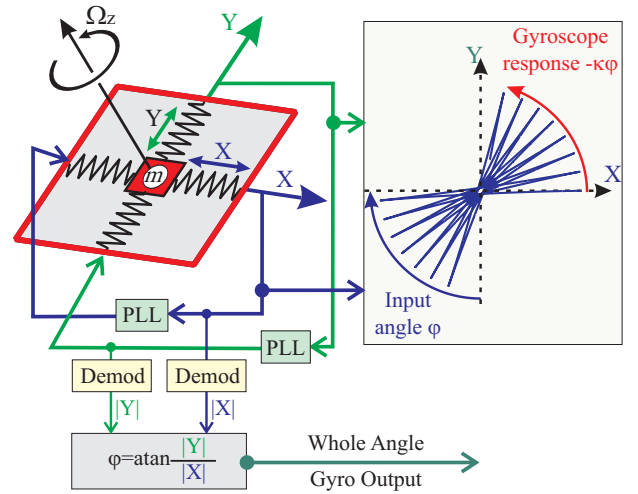


Fig. 11. Schematic and operating principle of a gyroscope for angle measurements (whole angle mode of operation). The axis of vibration is allowed to precess freely in response to the inertial rotation. The precession angle proportional to the angle of input rotation with the coefficient  $\kappa$ .

very wide sensor input range, limited only by the device natural frequency (for  $\Omega_z < \omega$ ). In order to experimentally investigate this hypothesis, a vacuum packaged QMG was mounted on an Ideal Aeromsmith High-Speed Position and Rate Table System 1571, and characterized from 0 to 18,000 %/s (i.e. 50 revolutions per second). Without any compensation, the FM gyroscope demonstrated less than 0.2% nonlinearity (limited by noise, not systematic nonlinearity) throughout the entire range, Figure 9.

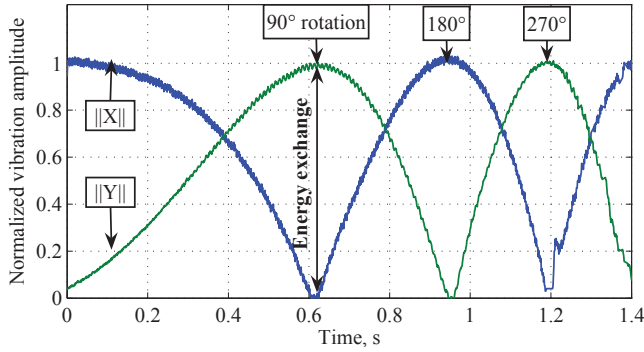
Noise performance of the FM sensor is limited by the frequency stability of the two modes of vibration in the gyroscope. Figure 10 demonstrates the Allan variance of the FM sensor, measurements showing a 1.6 %/hr ARW and 27 %/hr bias instability, resulting in a dynamic range of 128 dB. Next, we demonstrate that the same principle of operation can be applied for direct angle measurements by adding an amplitude demodulation step to extract instantaneous rotation angle  $\Omega_z t$  from (4).

## V. WHOLE ANGLE MODE

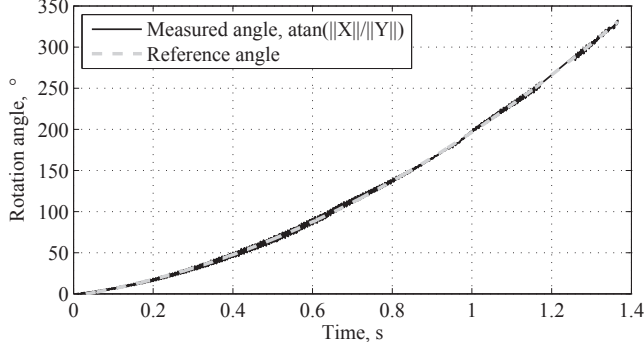
This section describes dynamics and experimental characterization of the QMG sensor operated in angle measuring mode [11]. The operating principle is based on free precession of the vibration axis in response to the inertial rotation, with the precession angle equal to the rotation angle.

### A. Whole-Angle (Rate Integrating) Dynamics

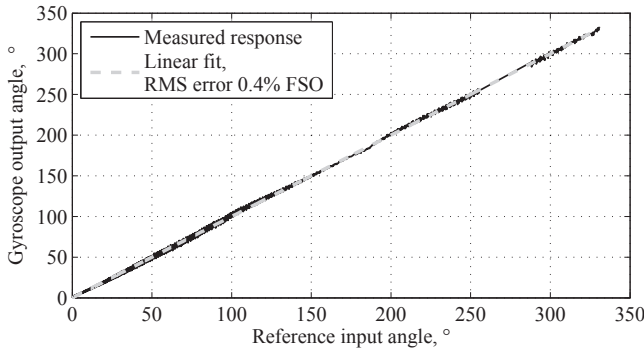
The whole-angle mode is based upon the classical Foucault pendulum operation, where the axis of vibration is allowed to precess freely in response to the inertial rotation. The dynamics is governed by the same Eq. (3) as in frequency modulated operation. The analytical solution shows that the trajectory pattern precesses with the angular rate  $-\Omega_z$  in the gyroscope frame, but remains fixed in the inertial space, thereby providing an inertial reference for orientation angle



(a) Measured vibration amplitudes of X- and Y- mode in response to rotation with constant acceleration  $280 \text{ }^\circ/\text{s}^2$ .



(b) Direct angle measurement derived from  $\arctan(y/x)/2$ .



(c) Measured angle response demonstrates sensor linearity.

Fig. 12. QMG angle response to a constant angular acceleration of  $280 \text{ }^\circ/\text{s}^2$  (input rates from 0 to  $450 \text{ }^\circ/\text{s}$ , or angular positions from 0 to  $350^\circ$  in 1.4 s).

measurements. In other words, at any time the variable inclination angle  $\theta$  of the orbital trajectory is equal to the angle of a gyroscope inertial rotation in  $x$ - $y$  plane (Fig. 11):

$$\theta = - \int_0^t \Omega_z(\tau) d\tau, \quad (7)$$

which proves that Foucault pendulum is a rate integrating gyroscope. The instantaneous changes in the precession angle  $\theta$  can be detected by monitoring  $x, y$  read-out displacements:

$$\theta = \arctan(y/x). \quad (8)$$

Unlike the conventional rate measuring mode, where the axis of vibration is locked to the intended drive direction, the whole-angle mode poses no practical limitation to the angular rate range or bandwidth [20]. This can be explained by the

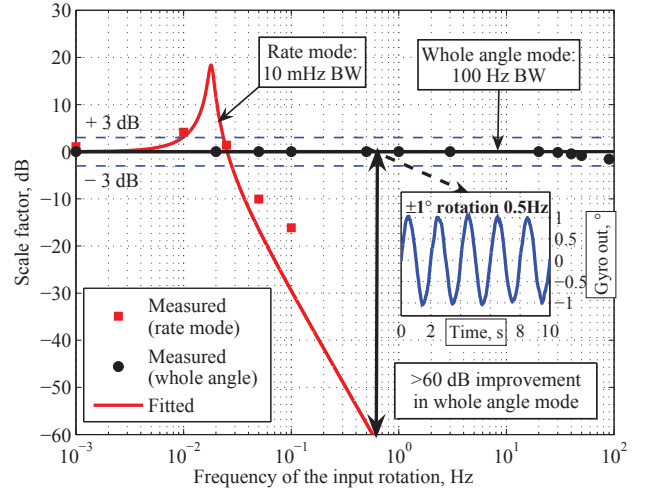


Fig. 13. Experimental comparison of the QMG sensor bandwidth up to 100 Hz range, demonstrating a 60 dB improvement when operated in the frequency modulated or whole-angle mode (in comparison to the conventional rate measuring mode).

free, unconstrained motion of the inertial mass. The ultimate maximum of the rotation rate and measurement bandwidth is defined by the resonant frequency of the device, which is approximately several kilohertz for a typical silicon MEMS vibratory gyroscope.

### B. Experimental Characterization

To demonstrate the whole-angle mode with fundamentally unlimited bandwidth and range, the QMG was operated in free vibrations. The device was rotated with a constant angular acceleration of  $280 \text{ }^\circ/\text{s}^2$ , providing input angular rates from 0 to  $450 \text{ }^\circ/\text{s}$ , or angular positions from 0 to  $350^\circ$  in 1.4 s, Fig. 12. The amplitude change of X- and Y-modes was recorded in response to a rotation with  $280 \text{ }^\circ/\text{s}^2$  angular acceleration, Fig. 12(a). Initially, the device was vibrating in X-direction, and after a  $90^\circ$  rotation the proof-mass was oscillating in the Y-direction. The subsequent  $90^\circ$  rotation causes the device to vibrate again in the X-mode. These energy transfers between the X- and Y-modes serve as the basis for the angle detection. The precession angle of the vibration pattern was computed in real time from the amplitudes of X- and Y-modes using the geometric relation  $\arctan(y/x)/2$ , Fig. 12(b). The measured angle response confirmed orientation-independent angular gain, and sensor linearity with 0.4% RMS error full scale output, Fig. 12(c). Experimental characterization of the whole-angle mode confirmed wide input range of  $450 \text{ }^\circ/\text{s}$  (limited by the experimental setup).

The whole-angle operating mode is also expected to provide unlimited measurement bandwidth. The bandwidth of mode-matched ultra-low dissipation QMG device was characterized for both conventional rate measuring (forced vibrations) and whole-angle modes (free vibrations). Scale factors were measured for periodic rotations with frequencies up to 100 Hz (limited by the setup). Scale factors of the rate operating mode were normalized to the constant rotation and compared to

the angular gain factors of the whole-angle mode, Fig. 13. Characterization of the whole-angle operating mode revealed a bandwidth in excess of 100 Hz, which is a 10,000 improvement over the conventional open-loop rate mode with a 10 mHz bandwidth (when operated with closely matched frequencies  $\Delta f$  of 20 mHz).

## VI. CONCLUSION

We demonstrated the interchangeable operation of a silicon MEMS Coriolis vibratory gyroscope capable of precision and wide range measurements of the angular rate and angle of rotation. The vacuum sealed SOI prototype with a 2 kHz operational frequency demonstrated virtually identical X- and Y-mode Q-factors of 1.2 million (with  $\Delta Q/Q$  of 1%), approaching the thermoelastic limit of 1.3 million. This allows for a power failure-independent operation with polarization voltages as low as 10 mV dc previously achieved only in HRG for space-flight missions [21]. Due to stiffness and damping symmetry, and ultra-low dissipation, this gyroscope was instrumented for the precision rate and angle measurements in high bandwidth and range. The QMG gyroscope experimentally demonstrated a 0.8 °/hr bias instability in rate measuring mode, a  $\pm 18,000$  °/s linear input range, and a 100 Hz measurement bandwidth (limited by the setup) in both whole-angle and frequency modulated modes. Temperature characterization of the transducer also revealed less than 0.2% variation of the angular rate response between 25 °C and 70 °C environments, enabled by the self-calibrating differential frequency detection. Interchangeable operation of the QMG transducer provides a measured 157 dB dynamic range with a 210 dB fundamental limit for a 2 kHz transducer, making one high-Q mechanical structure suitable for demanding high precision and wide input range applications.

## ACKNOWLEDGMENT

This work was supported by the Office of Naval Research and Naval Surface Warfare Center Dahlgren Division under Grants N00014-09-1-0424 and N00014-11-1-0483. The authors would like to thank the staff of the UCLA Nanoelectronics Research Facility and SST International for assistance with fabrication and vacuum packaging, Dr. Flavio Heer from Zurich Instruments AG for assistance with the signal processing, and Ilya Chepurko for assistance with the front-end PCB. The gyroscopes were designed and characterized at the MicroSystems Laboratory, University of California, Irvine.

## REFERENCES

- [1] A. M. Shkel, "Type I and Type II micromachined vibratory gyroscopes," in *Proc. IEEE/ION Position Locat. Navigat. Symp.*, San Diego, CA, Apr. 24–27, 2006, pp. 586–593.
- [2] D. Lynch, "Coriolis vibratory gyros," in *Symposium Gyro Technology*, Stuttgart, Germany, Sep. 15–16, 1998, pp. 1.0–1.14.
- [3] A. Shkel, "Microtechnology comes of age," *GPS World*, pp. 43–50, 2011.
- [4] M. Zaman, A. Sharma, Z. Hao, and F. Ayazi, "A mode-matched silicon-yaw tuning-fork gyroscope with subdegree-per-hour allan deviation bias instability," *Microelectromechanical Systems, Journal of*, vol. 17, no. 6, pp. 1526–1536, dec. 2008.

- [5] B. R. Johnson, E. Cabuz, H. B. French, and R. Supino, "Development of a mems gyroscope for northfinding applications," in *Position Location and Navigation Symposium (PLANS), 2010 IEEE/ION*, may 2010, pp. 168–170.
- [6] E. Tatar, S. Alper, and T. Akin, "Effect of quadrature error on the performance of a fully-decoupled mems gyroscope," in *Micro Electro Mechanical Systems (MEMS), 2011 IEEE 24th International Conference on*, jan. 2011, pp. 569–572.
- [7] I. Prikhodko, S. Zotov, A. Trusov, and A. Shkel, "Sub-degree-per-hour silicon MEMS rate sensor with 1 million Q-factor," in *Proc. 16th International Conference on Solid-State Sensors, Actuators and Microsystems (TRANSDUCERS'11)*, Beijing, China, Jun. 5–9, 2011, pp. 2809–2812.
- [8] F. Ayazi, "Multi-DOF inertial MEMS: From gaming to dead reckoning," in *Solid-State Sensors, Actuators and Microsystems Conference (TRANSDUCERS), 2011 16th International*, june 2011, pp. 2805–2808.
- [9] A. Trusov, I. Prikhodko, S. Zotov, A. Schofield, and A. Shkel, "Ultra-high Q silicon gyroscopes with interchangeable rate and whole angle modes of operation," in *Proc. Sensors, 2010 IEEE*, 2010, pp. 864–867.
- [10] S. Zotov, A. Trusov, and A. Shkel, "Experimental demonstration of a wide dynamic range angular rate sensor based on frequency modulation," in *Proc. IEEE Sensors 2011*, Limerick, Ireland, Oct. 28–31, 2011.
- [11] I. Prikhodko, S. Zotov, A. Trusov, and A. Shkel, "Foucault pendulum on a chip: Angle measuring silicon MEMS gyroscope," in *Proc. IEEE Int. Conf. Micro-Electro-Mechanical Systems*, Cancun, Mexico, Jan. 23–27, 2011, pp. 161–164.
- [12] S. Zotov, I. Prikhodko, A. Trusov, and A. Shkel, "Frequency modulation based angular rate sensor," in *Proc. IEEE Int. Conf. Micro-Electro-Mechanical Systems*, Cancun, Mexico, Jan. 23–27, 2011, pp. 577–580.
- [13] A. A. Trusov, A. R. Schofield, and A. M. Shkel, "Micromachined tuning fork gyroscopes with ultra-high sensitivity and shock rejection," U.S. Patent Application 20100313657.
- [14] A. Schofield, A. Trusov, and A. Shkel, "Versatile vacuum packaging for experimental study of resonant mems," in *Proc. Micro Electro Mechanical Systems (MEMS), 2010 IEEE 23rd International Conference on*, 2010, pp. 516–519.
- [15] L. Dong and D. Avanesian, "Drive-mode control for vibrational MEMS gyroscopes," *Industrial Electronics, IEEE Transactions on*, vol. 56, no. 4, pp. 956–963, april 2009.
- [16] J. Gregory, J. Cho, and K. Najafi, "MEMS rate and rate-integrating gyroscope control with commercial software defined radio hardware," in *Solid-State Sensors, Actuators and Microsystems Conference (TRANSDUCERS), 2011 16th International*, june 2011, pp. 2394–2397.
- [17] R. Antonello, R. Oboe, L. Prandi, and F. Biganzoli, "Automatic mode matching in MEMS vibrating gyroscopes using extremum-seeking control," *Industrial Electronics, IEEE Transactions on*, vol. 56, no. 10, pp. 3880–3891, oct. 2009.
- [18] A. Seshia, R. Howe, and S. Montague, "An integrated microelectromechanical resonant output gyroscope," in *Micro Electro Mechanical Systems, 2002. The Fifteenth IEEE International Conference on*, 2002, pp. 722–726.
- [19] C. Comi, A. Corigliano, G. Langfelder, A. Longoni, A. Tocchio, and B. Simoni, "A high sensitivity uniaxial resonant accelerometer," in *Micro Electro Mechanical Systems (MEMS), 2010 IEEE 23rd International Conference on*, jan. 2010, pp. 260–263.
- [20] D. Lynch, "Vibratory gyro analysis by the method of averaging," in *Proc. 2nd St. Petersburg International Conference on Gyroscopic Technology and Navigation*, 1995, pp. 26–34.
- [21] D. M. Rozelle, "The hemispherical resonator gyro: From wineglass to the planets (AAS 09-176)," in *Proc. 19th AAS/AIAA Space Flight Mechanics Meeting*, Feb. 2009, pp. 1157–1178.